Experimental Neurology 229 (2011) 332–338

Contents lists available at ScienceDirect

Experimental Neurology

journal homepage: www.elsevier.com/locate/yexnr

Granule cell dispersion in temporal lobe epilepsy is associated with changes in dendritic orientation and spine distribution

Thomas M. Freiman [a,*], Jessica Eismann-Schweimler [a], Michael Frotscher [b,c]

[a] Department of Neurosurgery, University Medical Center, Albert-Ludwigs-University Freiburg, D-79106 Freiburg, Germany
[b] Center of Neuroscience, Albert-Ludwigs-University Freiburg, D-79104 Freiburg, Germany
[c] Institute of Anatomy and Cell Biology, Albert-Ludwigs-University Freiburg, D-79104 Freiburg, Germany

ARTICLE INFO

Article history:
Received 8 December 2010
Revised 16 February 2011
Accepted 20 February 2011
Available online 1 March 2011

Keywords:
Temporal lobe epilepsy
Ammon's horn sclerosis
Hippocampus
Reelin
Granule cell
Dendrite
Spine

ABSTRACT

Granule cell dispersion is a characteristic feature of Ammon's horn sclerosis in temporal lobe epilepsy. It was recently shown that granule cell dispersion is associated with decreased expression of the extracellular matrix protein Reelin. Reelin controls neuronal lamination and the differentiation of dendrites and spines. Here, we studied dendritic orientation and the distribution of dendritic spines on granule cells in surgical specimens of patients suffering from temporal lobe epilepsy. In this material, we compared granule cells in dentate areas showing granule cell dispersion with granule cells in areas exhibiting a normal, densely packed granule cell layer. Granule cells (GC) were Golgi-stained and analyzed using a computer-based camera lucida system and were categorized as being located proximal or distal to the hilus (GCprox, GCdist). We found that GCprox in a densely packed granule cell layer exhibited a mainly vertically oriented dendritic arbor with a small bifurcation angle (17°) between branching dendrites. In contrast, GCdist in a densely packed granular layer showed a wider bifurcation angle (35°), suggesting a widening of the dendritic field during the migratory process to superficial positions. Granule cells in the dispersed granule cell layer showed an even wider bifurcation angle of their apical dendrites (GCprox: 40°; GCdist: 58°) and also exhibited recurrent basal dendrites. Spine density on dendrites of GCprox in dispersed areas was increased compared to GCprox in the normal, compact granule cell layer. In contrast, dendrites of GCdist extending into the molecular layer showed a reduced spine density in dispersed areas. The results are discussed in view of other findings on neuronal reorganization in the epileptic dentate gyrus.

Introduction

Temporal lobe epilepsy (TLE) is the most common type of pharmacoresistant epilepsy. It is characterized by neuronal loss and glial hypertrophy in the hippocampus, traditionally known as Ammon's horn sclerosis. Neuronal loss mainly involves pyramidal neurons in hippocampal region CA1 and in the hilus of the dentate gyrus (Sommer, 1880; Bratz, 1899; Mathern et al., 1997), largely sparing the CA3 region and the dentate granule cell layer (GCL). However, the dentate gyrus is the site of an extensive axonal reorganization in TLE. Having lost their target neurons, the mossy cells of the hilar region, the granule cell (GC) axons, the mossy fibers, sprout backwards into the GCL and inner molecular layer (Sutula et al., 1989). Furthermore, at many places the compact lamination of the granule cells is lost resulting in granule cell dispersion (GCD; Houser, 1990). Evidence has been provided that GCD develops in response to local deficiencies in the extracellular matrix protein Reelin (Haas et al., 2002; Heinrich et al., 2006). Reelin, a molecule important for layer formation during development, appears to control the maintenance of dentate architecture in the mature brain (Frotscher, 2010).

Here we studied to what extent GCD results in secondary changes in dendritic organization and the distribution of dendritic spines, major postsynaptic elements of excitatory synapses. The GCs of the dentate gyrus represent a gate to the rest of the hippocampus, and TLE-induced changes in their dendritic organization and afferent innervation are likely to affect hippocampal function (Buckmaster et al., 2000, 2002; Sloviter, 1994; Sloviter et al., 2006). At present, little is known about TLE-specific morphological changes in GCs since such changes are difficult to determine in view of the large variability of the GCs in primates when compared to rodents (Seress and Frotscher, 1990). Scheibel et al. (1974) observed atrophy of the dendritic tree with the formation of varicosities and a loss of spines in patients with TLE. Von Campe et al. (1997) showed an increase in length and complexity of apical dendrites in the inner molecular layer in GCs of patients with AHS, and Isokawa (1997) observed that the dendrites

Abbreviations: GC, granule cell; GCdist, GC located distal to the hilus; GCprox, GC located proximal to the hilus; GCD, granule cell dispersion; GCL, granule cell layer; GCLdisp, dispersed GCL; GCLnorm, normal compact GCL; TLE, temporal lobe epilepsy.

* Corresponding author at: Department of Neurosurgery, University Medical Center, Breisacher Str. 64, D-79106 Freiburg, Germany. Fax: +49 761 270 5022.
E-mail address: thomas.freiman@uniklinik-freiburg.de (T.M. Freiman).

0014-4886/$ – see front matter © 2011 Elsevier Inc. All rights reserved.
doi:10.1016/j.expneurol.2011.02.017

of GCs contacted by recurrent mossy fiber collaterals exhibited an increased spine density. In a mouse model of TLE, Suzuki et al. (1997) found a moderate increase in spine number and dendritic length in dendritic portions that were innervated by recurrent mossy fiber collaterals. Ribak and co-workers described the occurrence of basal dendrites in epileptic animals (Spigelman et al., 1998; Ribak et al., 2000).

To examine potential changes in dendritic organization and the distribution of spines in GCD, we compared GCs in intact portions of the dentate gyrus with GCs in dispersed regions in hippocampal specimens of patients with TLE who underwent surgery for therapeutic reasons. This approach was chosen in view of the difficulties in obtaining comparable control material from patients not suffering from epilepsy. We provide evidence for differences in both dendritic orientation and spine distribution between GCs in a virtually normal and in the dispersed dentate gyrus.

Materials and methods

Patient selection

Patients with TLE were treated according to the epilepsy surgery program of the University Medical Center Freiburg and underwent selective amygdalo-hippocampectomy or 2/3 temporal lobectomy with amygdalo-hippocampectomy (Table 1). In all patients, the removal of the hippocampus was warranted to achieve seizure control. Presurgical assessment consisted of documentation of detailed seizure history, neurological examination, and neuropsychological testing. Invasive and non-invasive long-term video electroencephalography monitoring as well as magnetic resonance imaging of the brain was performed. All patients experienced pharmacoresistant complex partial seizures. In all cases, the hippocampus was involved in the epileptogenic area. Informed consent was obtained from patients and families according to the Declaration of Helsinki. The Ethics Committee of the Albert-Ludwigs-University Freiburg approved the selection process and procedures (File no.: 100020/09).

Neuropathological examination of specimens from patients with temporal lobe epilepsy

Hippocampal specimens of TLE patients were graded qualitatively according to the classification of Wyler (Hermann et al., 1992): Grade I: mild damage, slight (<10%) or no neuronal loss in CA1 and CA3; grade II: moderate damage, gliosis, and moderate neuronal loss (10–20%) in CA1 and CA3; grade III: severe damage, gliosis with >50% neuronal loss in CA1 and CA3, but sparing CA2; grade IV: severe damage, gliosis with >50% neuronal loss involving all sectors of the hippocampal pyramidal cell layer. The fascia dentata, subiculum and parahippocampal gyrus may also be affected in grade IV patients. No significant relationship between seizure frequency and Wyler Grade was observed.

Tissue preparation

Human hippocampal surgical specimens were fixed by immersion in a solution containing 1% glutaraldehyde, 1% paraformaldehyde, and 15% saturated picric acid in 0.1 M phosphate buffer (pH 7.3). The tissue was stored in the fixative for extended periods of time. Thereafter, transverse sections of the hippocampus were cut on a vibratome (VT 1000 S, Leica, Bensheim, Germany; 100 μm), and the sections were processed either for cresyl violet staining or were Golgi-impregnated as described (Frotscher, 1992).

Quantitative analysis of granule cell layer width

Granule cell lamination was determined in cresyl violet-stained sections of the hippocampus. For this, sections were mounted on gelatin-coated slides, immersed in 0.1% cresyl violet solution for 10 min, dehydrated in increasing concentrations of ethanol, and coverslipped in Hypermount. In five consecutive sections, five measurements of GCL width were performed at 25 μm intervals (Haas et al., 2002; Houser, 1990) using AxioVision software (Carl Zeiss AG, Oberkochen, Germany). Statistical analysis included the mean and a 95% confidence interval (CI_{95}) as well as a rank correlation analysis (Spearman, 1904). Material from 10 patients was used for the present study. In the present study, the mean width of the GCL was 153 μm (range 51 μm up to 230 μm). In accordance with previous studies (Haas et al., 2002; Houser, 1990) a GCL width of 160 μm and more was considered as GCD.

Golgi impregnation

Tissue sections (100 μm) were processed according to the "sandwich" Golgi technique described in detail elsewhere (Frotscher,

Table 1
Patient data.

Pat. No.	Age [yr]	Sex	Seizure onset [yr]	Seizure rate/month	Seizure type	Relevant clinical history	Operation	Seizure outcome	Pathology	Slices/pat. (GCs/pat.) [n]	Mean GCD width [μm]
1	40	F	33	2	PS, SG	Febrile seizure	sAHE L	Engel I	AHS Wyler IV	5 (17)	159
2	39	M	16	4	PS, SG	None	sAHE L	Engel I	AHS Wyler IV	1 (4)	192
3	31	F	3	15	PS, SG	Meningitis of unknown origin	2/3 Temp.Res. R	Engel I	Temp. atrophy, AHS Wyler III	3 (14)	149
4	33	F	20	2	PS, SG	None	sAHE R	Engel I	AHS Wyler III	6 (21)	202
5	50	F	13	4	PS, SG	None	sAHE L	Engel I	AHS Wyler III	1 (1)	178
6	38	F	5	1	PS, SG	None	2/3 Temp.Res. R	Engel II	AHS Wyler III	1 (2)	180
7	34	M	5	12	PS, SG	Febrile seizure	2/3 Temp.Res. R	Engel III	FCD temp., AHS Wyler IV	2 (3)	171
8	43	M	18	15	PS, SG	None	sAHE L	0	AHS Wyler IV	4 (33)	230
9	46	M	3	5	PS	Prolonged birth	sAHE R	Engel I	Hamartoma, AHS Wyler I	1 (4)	121
10	43	M	38	10	PS	None	sAHE L	Engel I	AHS Wyler III	2 (6)	225

Abbreviations: F: female, M: male, PS: partial seizures, SG: secondary generalized seizures, sAHE: selective amygdalohippocampectomy, 2/3 Temp.Res.: two-third temporal lobe resection incl. amygdalohippocampectomy, R/L: right/left hemisphere, AHS: Ammon's horn sclerosis, FCD: focal cortical dysplasia, Engel I–IV: Engel outcome scale (I: free of disabling seizures, II: rare disabling seizures, III: worthwhile improvement, IV: no worthwhile improvement, 0: patient did not appear on postoperative control examination.

1992). Briefly, 10 hippocampal sections were piled on top of each other with intervening parafilm. The resulting block was embedded in 5% agar and immersed in an osmium dichromate solution for five days at 4 °C followed by incubation in 0.75% silver nitrate for 36–42 h at room temperature. After removal of the agar and dehydration the staining intensity was controlled under the light microscope. Non-impregnated sections were rehydrated, de-stained in 1% sodium thiosulphate solution, and impregnated again.

Classification, morphometric and statistical analysis of granule cells

Granule cells were classified into four groups, depending on their location in the normal or dispersed GCL (Fig. 1A). A first group consisted of GCs located in the normal (compact) GCL, close to the hilus (GCprox, Fig. 1A); a second group comprised GCs located distally to the hilus (GCdist, Fig. 1A). Groups three and four consisted of GCs in dispersed areas, again differentiated into GCprox and GCdist. The diameter of the GCL was measured individually for each GC at the location of the cell body (Fig. 1A). In addition, the distance between the hilus/GCL border and the base of the GC was measured. As a parameter of the lateral extension of the dendritic arbor, the angle between the outermost dendrites was measured.

For morphometric analysis of individual, Golgi-stained GCs, a series of concentric rings (distance 10 μm, Fig. 1B) were virtually centered around the cell body (Sholl, 1953) by using automated digital software Neurolucida 5.04.3 (Micro Bright Field, Inc., Williston, U.S.A.). The entire dendritic arbor was quantified by scanning the whole cell and using the Neurolucida program. The total length of dendrites and the number of spines per Sholl segment were analyzed for each neuron. Only visible lateral spines, but not spines in the anterior/posterior direction, were counted.

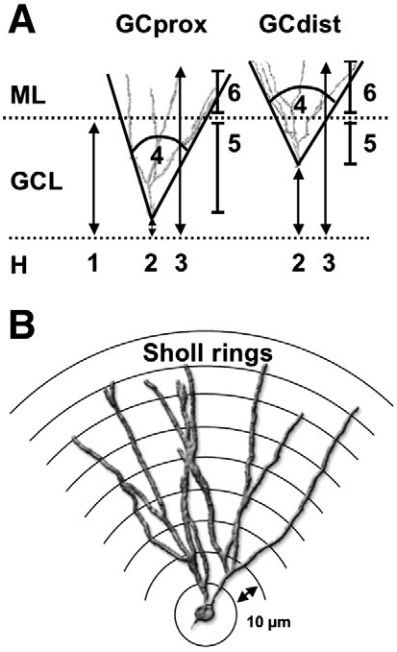

Fig. 1. *Schematic diagram of granule cell morphometric analysis.* (A) classification of granule cells (GCs) by estimation of the following parameters: (1) diameter of the granule cell layer (GCL); (2) distance of the GC from the hilus/GCL border to the base of the cell body; (3) distance from the hilus/GCL border (lower dotted line) to dendritic terminals (4) angle formed between bifurcating outer GC dendrites. Parameters (1) and (2) allowed for the classification of GCs as being located proximally or distally to the hilus (GCprox and GCdist, respectively). Parameter (3) allowed for the estimation of dendritic length within the GCL (5) and molecular layer (ML, 6). (B) Measurements of dendritic length and spine density were performed by means of a Sholl analysis (Sholl, 1953). The distance between each ring was 10 μm.

Statistical analysis included the mean, standard deviation (SD) and the 95% confidence interval (CI_{95}). Differences were considered statistically significant with $p<0.05$, using the two-sample Wilcoxon rank-sum test.

Results

Granule cell dispersion

The extent of GCD was found to vary within individual tissue samples (Figs. 2A, B). For all GCprox in non-dispersed areas the mean width of the GCL amounted to 111 μm (CI_{95} = 118 μm, 104 μm; n = 31) and to 118 μm in GCdist (CI_{95} = 129 μm, 108 μm; n = 31). In contrast, the mean width of the GCL in dispersed areas amounted to 187 μm for GCprox (CI_{95} = 198 μm, 177 μm; n = 21) and to 213 μm for GCdist (CI_{95} = 224 μm, 203 μm; n = 17). The GCL width was significantly different between GCs of dispersed and non-dispersed areas ($p<0.0001$), whereas it was not different when proximally and distally located GCs in each of these regions were compared.

Morphology and orientation of dendrites

Proximal GCs in non-dispersed areas had a vertically orientated ovoid cell body from which one or two apical dendrites extended into the molecular layer (Fig. 3A). The main apical dendrites bifurcated when they had passed superficial GCs; the mean number of their dendrites amounted to 2.1 (CI_{95} = 2.3, 1.9; n = 31). Basal dendrites were virtually absent (mean = 0.3; CI_{95} = 0.5, 0.1; n = 31). The dendritic arbor was

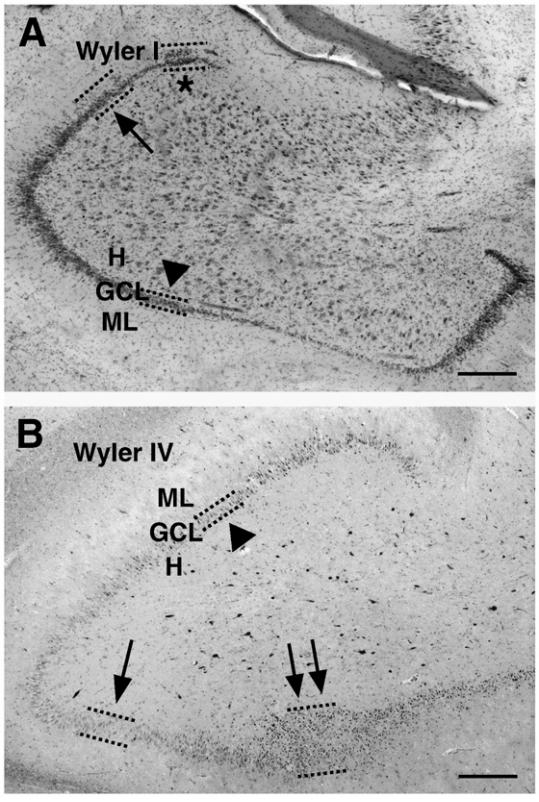

Fig. 2. *Differences in the extent of granule cell dispersion in the dentate gyrus.* (A) nearly normal hippocampus (Wyler grade I) without major cell loss and prominent GCD. However, some portions of the GCL show dispersed granule cells. Arrowhead marks a compact portion of the GCL; arrow points to a dispersed portion. The asterisk indicates a segment of the GCL that displays a doubled layer. (B) sclerotic hippocampus (Wyler grade IV). Note significant cell loss in the hilar region (H). arrowhead marks a compact portion of the GCL, while the arrow points to a dispersed portion. The double arrow labels a severely dispersed segment of the GCL. Scale bars 500 μm.

vertically orientated and the mean angle between outermost dendrites amounted to 17° (CI_{95} = 20°, 14°; n = 31; Fig. 4). Distal GCs in non-dispersed segments of the GCL showed a more widespread dendritic arbor (Fig. 3C). They usually gave rise to two or more dendrites (mean = 2.4; CI_{95} = 2.6, 2.1; n = 31); basal dendrites were rare (mean = 0.2; CI_{95} = 0.4, 0.0; n = 31). Of note, the mean angle between outermost apical dendrites was larger than in GCprox (35°; CI_{95} = 41°, 29°; n = 31; $p<0.0001$, Fig. 4).

In dispersed portions of the dentate gyrus, GCprox still showed a vertical dendritic orientation (Fig. 3B), but displayed significantly more apical dendrites than their counterparts in the compact GCL (mean = 2.5; CI_{95} = 2.8, 2.3; n = 26; $p = 0.01$) and gave rise to recurrent basal dendrites (mean = 0.4; CI_{95} = 0.6, 0.2; n = 26; Fig. 3B). The spread of the dendritic tree amounted to a mean angle of 40° (CI_{95} = 45°, 35°; $p<0.0001$, n = 26; Fig. 4) and was thus significantly increased when compared to GCprox in non-dispersed portions of the dentate gyrus ($p<0.01$). In GCdist of dispersed portions of the GCL (Fig. 3D), the number of dendrites was highest, amounting to a mean of 2.8 (CI_{95} = 3.2, 2.4; n = 17, $p = 0.04$). In contrast, basal dendrites were very rare (mean = 0.1; CI_{95} = 0.2, −0.1; n = 17). The dendritic tree was significantly more horizontally oriented than in GCdist of the non-dispersed GCL, forming an angle of 58° (CI_{95} = 70°, 46°; n = 17; $p<0.0001$; Fig. 4).

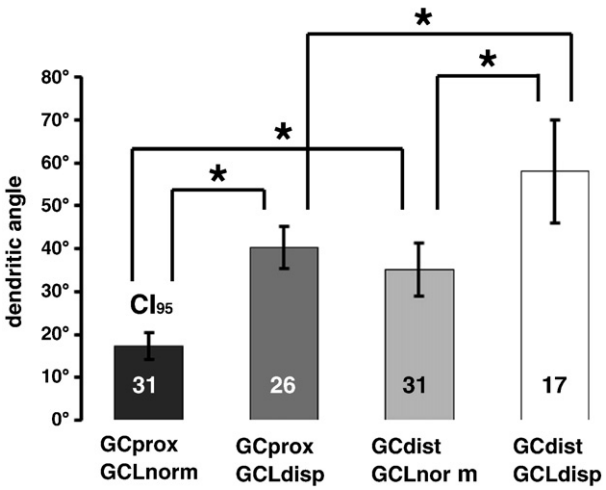

Fig. 4. *Angles formed by bifurcating outer dendrites.* The dendritic angle of GCdist is significantly enlarged compared to GCprox. Both GC types show an enlargement of their dendritic angle in GCLdisp compared to GCLnorm. Asterisks indicate statistically significant differences ($p<0.05$).

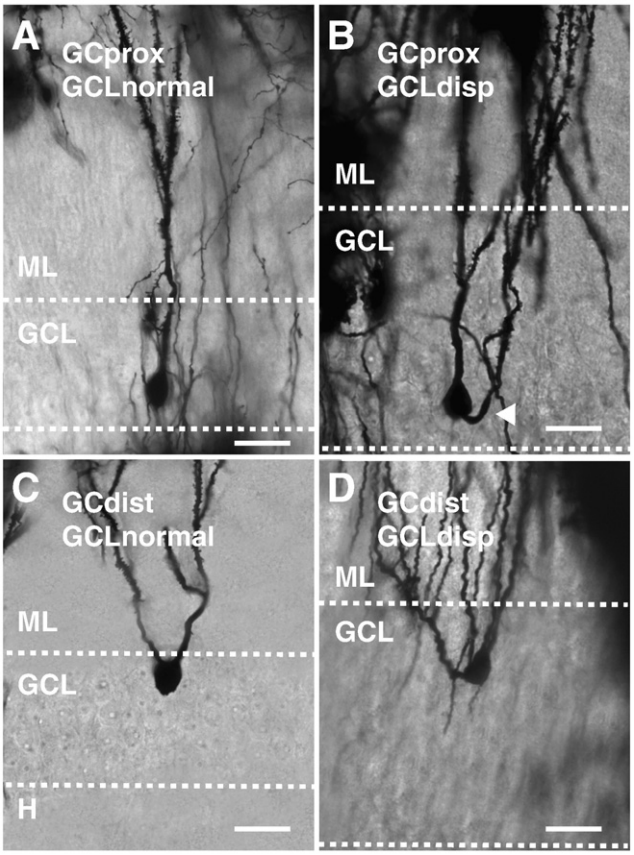

Fig. 3. *Differences in the angle of Golgi-impregnated granule cell dendrites in the normal and the dispersed granule cell layer.* (A) granule cell, located proximally (GCprox) to the hilus (H) in a normal, non-dispersed portion of the GCL (GCLnormal), showing a vertical orientation of its dendrites. Dotted lines demarcate GCL borders. There are only few spines on proximal dendritic segments in the GCL, whereas the spine density increases on dendritic segments in the ML. (B) GCprox located in the dispersed GCL (GCLdisp) with a recurrent basal dendrite (arrowhead). Many spines are visible on dendrites traversing the GCL. (C) Granule cell located distally to the hilus (GCdist) in the normal compact GCL. There are numerous spines on dendrites in the ML. (D) GCdist in the dispersed GCL. Note greater horizontal spread of dendrites. Spines on dendrites in the ML are sparse. Scale bars: 10 µm.

Spine density

Granule cells in the normal, compact GCL were found to have a characteristic spine distribution along the dendritic tree, with a low spine density on dendritic segments inside the GCL and a high density in the ML (Figs. 3, 5). In GCD, this characteristic distribution was altered. Thus, the spine density along dendritic segments of GCprox traversing the GCL amounted to 0.10 spines/µm (CI_{95} = 0.15 spines/µm, 0.05 spines/µm; n = 16, Fig. 5) in compact portions of the GCL and to 0.27 spines/µm in the dispersed GCL (CI_{95} = 0.33 spines/µm, 0.20 spines/µm; n = 14; $p<0.01$). In the ML, spine density of GCprox was not significantly different between GCs in dispersed and non-dispersed regions (0.23 spines/µm in the normal GCL; CI_{95} = 0.31 spines/µm, 0.14 spines/µm; n = 16, and 0.28 spines/µm in the dispersed GCL; CI_{95} = 0.40 spines/µm, 0.16 spines/µm; n = 14). Average spine density of all dendritic segments in GCprox amounted to 0.19 spines/µm (CI_{95} = 0.26 spines/µm, 0.12 spines/µm; n = 16) in

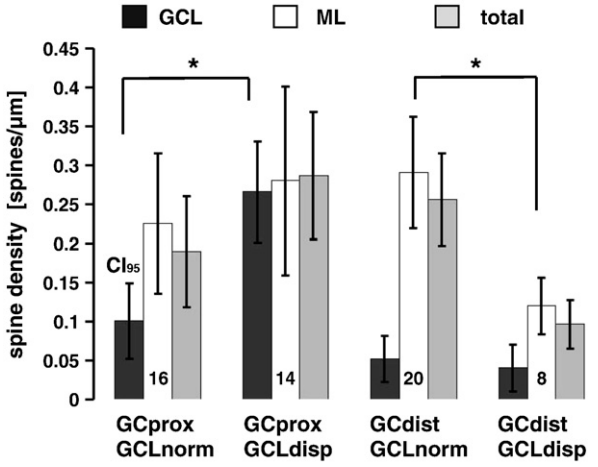

Fig. 5. *Spine densities on granule cell dendrites.* In the non-dispersed GCL (GCLnorm) proximal granule cells (GCprox) show a low spine density in the GCL and a high spine density in the ML. In GCLdisp this turned into the opposite and GCprox show an increase in spine density in the GCL. GCdist in GCLnorm show a low spine density in the GCL and a high spine density in the ML; this turns into the opposite in GCLdisp, where there is a decrease of spine density in the ML. Asterisks indicate statistically significant differences ($p<0.05$).

the normal, compact GCL and to 0.29 spines/μm in the dispersed GCL (CI_{95} = 0.37 spines/μm, 0.21 spines/μm; n = 14).

Interestingly enough, GCdist showed a significant decrease in the density of spines on dendrites in the ML of the dispersed dentate when compared to their counterparts in the normal compact GCL (0.29 spines/μm; CI_{95} = 0.36 spines/μm, 0.22 spines/μm; n = 20, versus 0.12 spines/μm; CI_{95} = 0.16 spines/μm, 0.08 spines/μm; n = 8). Accordingly, average spine density on GCdist was significantly decreased in the dispersed GCL, amounting to 0.10 spines/μm (CI_{95} = 0.13 spines/μm, 0.07 spines/μm; n = 8) compared to 0.26 spines/μm (CI_{95} = 0.31 spines/μm, 0.20 spines/μm; n = 20) in the non-dispersed GCL. On dendrites within the GCL, spine densities were not different between GCdist in dispersed and non-dispersed portions of the GCL (0.05 spines/μm in the compact GCL; CI_{95} = 0.08 spines/μm, 0.02 spines/μm; n = 20, and 0.04 spines/μm; CI_{95} = 0.07 spines/μm, 0.01 spines/μm; n = 8). A Spearman rank correlation analysis confirmed these findings. GCprox showed a significantly increased spine density that correlated with the extent of dispersion (Fig. 6; $p<0.01$). Similarly, the decreased spine density in GCdist correlated with the extent of GCD ($p<0.01$).

The dendritic length did not differ significantly between the four GC types, it amounted to 497 μm (CI_{95} = 722 μm, 272 μm, n = 16) in GCprox in compact GCL, 514 μm (CI_{95} = 714 μm, 314 μm; n = 14) in GCprox in dispersed GCL, 569 μm (CI_{95} = 793 μm, 345 μm, n = 20) in GCdist in compact GCL, 618 μm (CI_{95} = 813 μm, 423 μm; n = 8) in GCdist in dispersed GCL.

Discussion

Granule cell dispersion is a characteristic structural abnormality in temporal lobe epilepsy (Houser, 1990). The normal dentate gyrus in the mammalian brain consists of a densely packed GCL. In contrast, in TLE as well as in animal models of the disease (Bouilleret et al., 1999; Heinrich et al., 2006), the GCs are more loosely distributed with many neurons located in the molecular layer and hilus, respectively. Although this abnormal location of the GCs shares similarities with a developmental migration defect as observed in the mouse mutant reeler deficient in the extracellular matrix protein Reelin (Stanfield and Cowan, 1979; Drakew et al., 2002), GCD in epilepsy does not appear to be a developmental defect, it can be reliably induced experimentally in animals by intrahippocampal injection of the glutamate receptor agonist kainate (Bouilleret et al., 1999; Heinrich et al., 2006). Following unilateral intrahippocampal injection, the animals develop recurrent seizures and GCD on the side of kainate injection but not on the contralateral side. It is reasonable to assume that GCD in human TLE develops in a similar way, resulting from excess glutamate release during seizures. Previous studies in experimental animals have provided evidence for the dispersion to be caused by a displacement or active migration of fully differentiated neurons (Heinrich et al., 2006; Fahrner et al., 2007). The results of the present study in tissue samples from epileptic patients show that this repositioning of the GCs is associated with changes in the dendritic orientation and in the distribution of spines on the dendrites of these neurons.

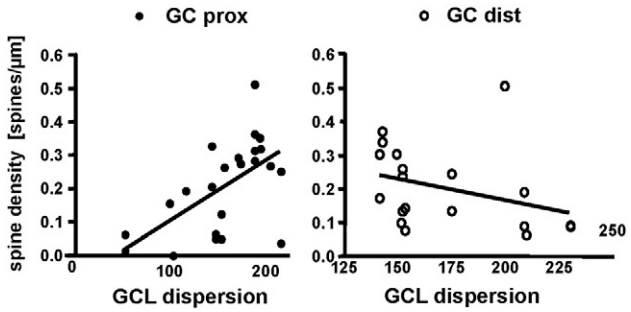

Fig. 6. *Spearman correlation of spine density and granule cell dispersion.* Proximal GCs show an increase whereas GCdist show a decrease in spines with increasing width of the GCL. Both correlations are significant ($p<0.01$).

Granule cell dispersion is induced by Reelin deficiency

In the reeler mutant deficient in Reelin, GCs do not assemble to form a compact GCL (Stanfield and Cowan, 1979; Drakew et al., 2002), indicating that Reelin is important for the normal lamination of the dentate gyrus. Of note, infusion of Reelin-blocking antibodies into the hippocampus of adult mice similarly resulted in a loss of compact GC lamination at the infusion site, i.e., it resulted in GCD, whereas infusion of neutral IgG had no effect (Heinrich et al., 2006). These findings indicate that Reelin is not only important for the formation but also for the maintenance of the differentiated dentate architecture (Frotscher, 2010). Along this line, in animals with unilateral intrahippocampal kainate injections, formation of GC dispersion on the injected side is accompanied by a loss of Reelin-synthesizing neurons on that side, but not on the contralateral side that shows normal Reelin expression and a compact GCL (Heinrich et al., 2006). Moreover, in tissue samples from human epileptic patients, the extent of GCD was found to correlate with a loss of Reelin-expressing neurons (Haas et al., 2002), and in the kainate model infusion of recombinant Reelin prevented GCD formation (Müller et al., 2009). Collectively, these data point to a role of Reelin in maintaining the laminated, compact organization of the dentate GCL.

Reelin is synthesized and secreted by Cajal–Retzius cells in the outer molecular layer, the marginal zone of the dentate gyrus (D'Arcangelo et al., 1995, 1997). It likely forms a gradient and stabilizes the cytoskeleton of the GCs and their dendrites. A recent study has in fact shown that Reelin stabilizes the actin cytoskeleton by phosphorylating cofilin (Chai et al., 2009). Cofilin is an actin-associated protein that disassembles F-actin, a mechanism that is required for changes in cell shape (Bamburg, 1999). Phosphorylation of cofilin renders the protein unable to disassemble F-actin, thereby stabilizing the cytoskeleton (Arber et al., 1998). The available data indicate that Reelin-induced cofilin phosphorylation prevents aberrant GC motility, and loss of Reelin in epilepsy results in enhanced neuronal motility leading to GCD.

Granule cell dispersion is associated with dendritic spread

Granule cells are generated in the secondary proliferation zone of the hilus and migrate from there to their destinations in the molecular layer. Unlike the layers of the neocortex, the dentate GCL forms in an outside-in fashion with early generated GCs occupying superficial, and late generated neurons deep portions of the GCL. Accordingly, most superficial GCs have migrated for the longest distance. The results of the present study clearly show that deeply located GCs (GCprox) have a vertically oriented dendritic arbor, whereas superficially located neurons give rise to a more widespread dendritic tree as reflected by a larger angle between bifurcating dendrites. Migration to the top of the GCL thus seems to be associated with a lateral extension of GC dendrites. Von Campe et al. (1997) showed indeed an increased length of dendritic segments in the inner molecular layer. This normal dendritic expansion during GC migration appears to be enhanced in GCD along with increased migratory activity of the GCs, resulting in an even larger angle between dendrites and an almost horizontal extension of the dendritic arbor. Preliminary data in slice cultures treated with kainate indicate that nuclear translocation into one of the ascending dendrites underlies this aberrant migration and the repositioning of GC dendrites, including the formation of recurrent basal dendrites (Chai et al., unpublished observations).

Changes in spine distribution in granule cell dispersion

The present results indicate that not only the dendritic arbor is subject to changes in GCD but also the distribution of spines along the

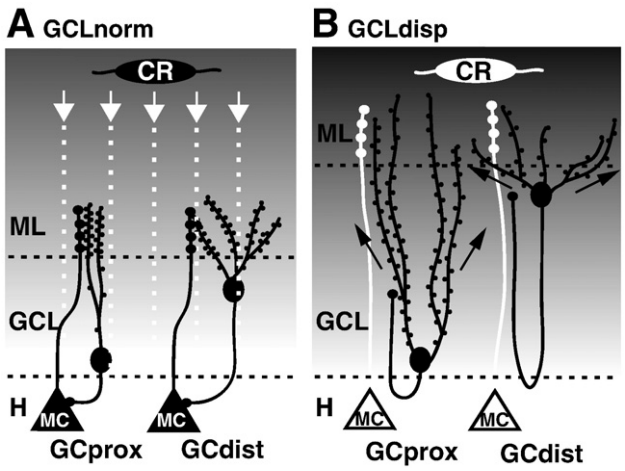

Fig. 7. *Schematic diagram of dendritic orientation and spine distribution in proximal and distal granule cells in the normal, compact and in the dispersed granule cell layer.* (A) proximal and distal GCs in the normal dentate gyrus innervate mossy cells (MC) in the hilus (H) by collaterals of mossy fibers (GC axons) They are kept in place by Reelin that is synthesized by Cajal–Retzius (CR) cells and forms a gradient in the ML (white arrows and white dotted lines). The angle between bifurcating dendrites is small in GCprox and more spread in GCdist. Dendrites within the GCL have few spines, whereas dendrites in the molecular layer are densely covered with spines. (B) epilepsy-induced local Reelin deficiency (indicated here by the lack of Cajal–Retzius cells) results in increased GC motility and granule cell dispersion (GCD) accompanied by a spread of the dendritic arbor in both GCprox and GCdist (black arrows). The epilepsy-induced loss of hilar mossy cells is associated with a loss of input to the proximal GC dendrites in the ML (degenerated MC axons), probably leading to decreased spine density there. This loss of innervation is partially compensated for by recurrent mossy fiber collaterals that are likely to contribute to an increased spine density of dendrites within the dispersed GCL.

GC dendrites. Two contrasting changes were observed: Superficially located GCs (GCdist) showed a reduced number of spines on their dendrites invading the molecular layer. In contrast, deeply located GCs (GCprox) showed an increased spine density on dendrites traversing the widened GCL. At present, it can only be speculated about the mechanisms underlying these changes in spine distribution (Fig. 7). It is firmly established that TLE results in a loss of hilar mossy cells known to impinge on GC dendrites in the ML (Blümcke et al., 2000). Loss of afferent innervation is likely to be followed by a loss of postsynaptic spines on GC dendrites in the ML, reminiscent of the spine loss on neurons in the visual cortex following visual deprivation or enucleation (Valverde, 1967, 1968). On the contrary, the increase in spine number on proximal dendrites in the GCL may reflect sprouting of mossy fibers (Suzuki et al., 1997). In TLE as well as in animal models of epilepsy, mossy fibers in the hilar region, having lost their postsynaptic partners, the mossy cells, sprout backwards, and innervate proximal GC dendrites (Sutula et al., 1989; Buckmaster et al., 2002; Isokawa et al., 1993; Sloviter et al., 2006). Isokawa (1997) showed indeed that recurrent mossy fiber collaterals impinged on proximal granule cell dendrites that exhibited an increased spine density. Taken together, it is likely that the supernumerous spines on proximal GC dendrites are indeed contacted by sprouting, recurrent mossy fiber collaterals.

Conclusions

The results of the present study confirm and extend previous findings, indicating that GCD in epilepsy results from an aberrant plasticity of differentiated GCs associated with GC relocation. This increased motility of the GCs is likely caused by deficient Reelin expression and cytoskeletal destabilization, respectively. The present results show that increased GC motility is accompanied by dendritic reorientation. Neuronal loss on the one hand, and mossy fiber sprouting on the other are likely to contribute to the observed changes in spine density along GC dendrites.

Acknowledgments

We thank Prof. Schulte-Mönting, Institute of Medical Biometry and Medical Informatics, for his help with the statistics, Dr. Alexander Drakew, Department of Neuroanatomy, for his help with the Golgi impregnations, Friederike Moos for excellent technical assistance and Prof. Marco Prinz for the neuropathological examination of the hippocampal specimens. These studies were supported by the Deutsche Forschungsgemeinschaft, TR-3, Project D6 to TMF and MF. MF was also supported by the Hertie Foundation.

References

Arber, S., Barbayannis, F.A., Hanser, H., Schneider, C., Stanyon, C.A., Bernard, O., et al., 1998. Regulation of actin dynamics through phosphorylation of cofilin by LIM-kinase. Nature 393, 805–809.
Bamburg, J.R., 1999. Proteins of the ADF/cofilin family: essential regulators of actin dynamics. Annu. Rev. Cell Biol. 15, 185–230.
Blümcke, I., Suter, B., Behle, K., Kuhn, R., Schramm, J., Elger, C.E., et al., 2000. Loss of hilar mossy cells in Ammon's horn sclerosis. Epilepsia 41, S174–S180.
Bouilleret, V., Ridoux, V., Depaulis, A., Marescaux, C., Nehlig, A., Le Gal La Salle, G., 1999. Recurrent seizures and hippocampal sclerosis following intrahippocampal kainate injection in adult mice: electroencephalography, histopathology and synaptic reorganization similar to mesial temporal lobe epilepsy. Neuroscience 89, 717–729.
Bratz, E., 1899. Ammonshornbefunde bei Epileptikern. Arch. Psychiatr. Nervenkr. 32, 820–835.
Buckmaster, P.S., Jongen-Relo, A.L., Davari, S.B., Wong, E.H., 2000. Testing the disinhibition hypothesis of epileptogenesis in vivo and during spontaneous seizures. J. Neurosci. 20, 6232–6240.
Buckmaster, P.S., Zhang, G.F., Yamawaki, R., 2002. Axon sprouting in a model of temporal lobe epilepsy creates a predominantly excitatory feedback circuit. J. Neurosci. 22, 6650–6658.
Chai, X., Förster, E., Zhao, S., Bock, H.H., Frotscher, M., 2009. Reelin stabilizes the actin cytoskeleton of neuronal processes by inducing n-cofilin phosphorylation at serine3. J. Neurosci. 29, 288–299.
D'Arcangelo, G., Miao, G.G., Chen, S.C., Soares, H.D., Morgan, J.I., Curran, T., 1995. A protein related to extracellular matrix proteins deleted in the mouse mutant reeler. Nature 374, 719–723.
D'Arcangelo, G., Nakajima, K., Miyata, T., Ogawa, M., Mikoshiba, K., Curran, T., 1997. Reelin is a secreted glycoprotein recognized by the CR-50 monoclonal antibody. J. Neurosci. 17, 23–31.
Drakew, A., Deller, T., Heimrich, B., Gebhardt, C., Del Turco, D., Tielsch, A., et al., 2002. Dentate granule cells in reeler mutants and VLDLR and ApoER2 knockout mice. Exp. Neurol. 176, 12–24.
Fahrner, A., Kann, G., Flubacher, A., Heinrich, C., Freiman, T.M., Zentner, J., et al., 2007. Granule cell dispersion is not accompanied by enhanced neurogenesis in temporal lobe epilepsy patients. Exp. Neurol. 203, 320–332.
Frotscher, M., 1992. Application of the Golgi/electron microscopy technique for cell identification in immunocytochemical, retrograde labeling, and developmental studies of hippocampal neurons. Microsc. Res. Tech. 23, 306–323.
Frotscher, M., 2010. Role for Reelin in stabilizing cortical architecture. Trends Neurosci. 33, 407–414.
Haas, C.A., Dudeck, O., Kirsch, M., Huszka, C., Kann, G., Pollak, S., et al., 2002. Role for reelin in the development of granule cell dispersion in temporal lobe epilepsy. J. Neurosci. 22, 5797–5802.
Heinrich, C., Nitta, N., Flubacher, A., Muller, M., Fahrner, A., Kirsch, M., et al., 2006. Reelin deficiency and displacement of mature neurons, but not neurogenesis, underlie the formation of granule cell dispersion in the epileptic hippocampus. J. Neurosci. 26, 4701–4713.
Hermann, B.P., Wyler, A.R., Somes, G., Berry III, A.D., Dohan Jr., F.C., 1992. Pathological status of the mesial temporal lobe predicts memory outcome from left anterior temporal lobectomy. Neurosurgery 31, 652–656.
Houser, C.R., 1990. Granule cell dispersion in the dentate gyrus of humans with temporal lobe epilepsy. Brain Res. 535, 195–204.
Isokawa, M., 1997. Preservation of dendrites with the presence of reorganized mossy fiber collaterals in hippocampal dentate granule cells in patients with temporal lobe epilepsy. Brain Res 1997;744:339–43. Erratum in. Brain Res. 758, 263.
Isokawa, M., Levesque, M.F., Babb, T.L., Engel Jr., J., 1993. Single mossy fiber axonal systems of human dentate granule cells studied in hippocampal slices from patients with temporal lobe epilepsy. J. Neurosci. 13, 1511–1522.
Mathern, G.W., Kuhlman, P.A., Mendoza, D., Pretorius, J.K., 1997. Human fascia dentata anatomy and hippocampal neuron densities differ depending on the epileptic syndrome and age at first seizure. J. Neuropathol. Exp. Neurol. 56, 199–212.
Müller, M.C., Osswald, M., Tinnes, S., Häussler, U., Jacobi, A., Förster, E., et al., 2009. Exogenous reelin prevents granule cell dispersion in experimental epilepsy. Exp. Neurol. 216, 390–397.
Ribak, C.E., Tran, P.H., Spigelman, I., Okazaki, M.M., Nadler, J.V., 2000. Status epilepticus-induced hilar basal dendrites on rodent granule cells contribute to recurrent excitatory circuitry. J. Comp. Neurol. 428, 240–253.
Scheibel, M.E., Crandall, P.H., Scheibel, A.B., 1974. The hippocampal-dentate complex in temporal lobe epilepsy. A Golgi study. Epilepsia 15, 55–80.

Seress, L., Frotscher, M., 1990. Morphological variability is a characteristic feature of granule cells in the primate fascia dentata: a combined Golgi/electron microscope study. J. Comp. Neurol. 293, 253–267.
Sholl, D.A., 1953. Dendritic organization in the neurons of the visual and motor cortices of the cat. J. Anat. 87, 387–406.
Sloviter, R.S., 1994. The functional organization of the hippocampal dentate gyrus and its relevance to the pathogenesis of temporal lobe epilepsy. Ann. Neurol. 35, 640–654.
Sloviter, R.S., Zappone, C.A., Harvey, B.D., Frotscher, M., 2006. Kainic acid-induced recurrent mossy fiber innervation of dentate gyrus inhibitory interneurons: possible anatomical substrate of granule cell hyper-inhibition in chronically epileptic rats. J. Comp. Neurol. 494, 944–960.
Sommer, W., 1880. Erkrankung des Ammonshorns als aetiologisches Moment der Epilepsie. Arch. Psychiatr. Nervenkr. 10, 631–675.
Spearman, C., 1904. "General Intelligence", objectively determined and measured. Am. J. Psychol. 15, 201–293.
Spigelman, I., Yan, X.-X., Obenaus, A., Lee, E.Y.-S., Wasterlain, C.G., Ribak, C.E., 1998. Dentate granule cells form novel basal dendrites in a rat model of temporal lobe epilepsy. Neuroscience 86, 109–120.
Stanfield, B.B., Cowan, W.M., 1979. The morphology of the hippocampus and dentate gyrus in normal and reeler mice. J. Comp. Neurol. 185, 393–422.
Sutula, T., Cascino, G., Cavazos, J., Parada, I., Ramirez, L., 1989. Mossy fiber synaptic reorganization in the epileptic human temporal lobe. Ann. Neurol. 26, 321–330.
Suzuki, F., Makiura, Y., Guilhem, D., Sorensen, J.C., Onteniente, B., 1997. Correlated axonal sprouting and dendritic spine formation during kainate-induced neuronal morphogenesis in the dentate gyrus of adult mice. Exp. Neurol. 145, 203–213.
Valverde, F., 1967. Apical dendritic spines and light deprivation in the mouse. Exp. Brain Res. 3, 337–352.
Valverde, F., 1968. Structural changes in the area striata of the mouse after enucleation. Exp. Brain Res. 5, 274–292.
von Campe, G., Spencer, D.D., de Lanerolle, N.C., 1997. Morphology of dentate granule cells in the human epileptogenic hippocampus. Hippocampus 7, 472–488.